In-plane magnetic penetration depth in NbS_2

P. Diener,[1] M. Leroux,[1] L. Cario,[2] T. Klein,[1,3] and P. Rodière[1]

[1]*Institut Néel, CNRS/UJF 25 rue des Martyrs, BP 166, F-38042 Grenoble cedex 9, France*

[2]*Institut des Matériaux Jean Rouxel (IMN), Université de Nantes, CNRS, 2 rue de la Houssinière, BP 3229, F-44322 Nantes, France*

[3]*Institut Universitaire de France and Université J. Fourier-Grenoble 1, Grenoble, France*

(Received 11 August 2010; revised manuscript received 17 May 2011; published 11 August 2011)

We report on the temperature dependence of the in-plane magnetic penetration depth (λ_{ab}) and first penetration field [$H_f \propto 1/\lambda_{ab}^2(T)$ for $H\|c$] in 2H-NbS_2 single crystals. An exponential temperature dependence is clearly observed in λ_{ab}(T) at low temperature, marking the presence of a fully open superconducting gap. This compound is the only superconducting 2H-dichalcogenide which does not develop a charge density wave (CDW). However, as previously observed in 2H-$NbSe_2$, this gap ($\Delta_1 = 1.1\,k_BT_c$) is significantly smaller than the standard BCS weak-coupling value. At higher temperature, a larger gap ($\Delta_2 = 1.8\,k_BT_c$) has to be introduced to describe the data which are compatible with a two-gap model. The superconducting gaps are hence very similar in NbS_2 and $NbSe_2$ and we show here that both of them open in the strongly coupled Nb tubular sheets independent of whether or not a CDW is present.

DOI: 10.1103/PhysRevB.84.054531 PACS number(s): 74.25.nn, 74.25.F−, 74.25.Ha, 74.70.Xa

I. INTRODUCTION

In numerous strongly correlated systems, superconductivity appears in the vicinity of a second electronic instability. These superconductors then often show deviations from the weak-coupling BCS theory, which raises the question of the interplay between the two orders.[1] This question is particularly well illustrated in dichalcogenides. Indeed, in 1T-$TiSe_2$,[2,3] 2H-TaS_2,[4,5] or 2H-$NbSe_2$ superconductivity coexists with a charge density wave (CDW). In 2H-$NbSe_2$ the charge density wave develops for instance at $T_D = 33$ K and coexists with superconductivity (SC) below $T_c = 7.1$ K.

In parallel, specific heat, tunneling spectroscopy, and de Haas–van Alphen measurements[6–10] showed that $NbSe_2$ is characterized by the coexistence of two superconducting gaps: $\Delta_1 = (1.0 \pm 0.1)k_BT_c$, which is much smaller than the BCS weak-coupling value ($\Delta/k_BT_c \sim 1.7$) and $\Delta_2 = (2.0 \pm 0.3)k_BT_c$. It was then initially suggested that the CDW might be at the origin of Δ_1.[11–14]

However, scanning tunneling spectroscopy (STS) and specific heat measurements clearly indicated the presence of a reduced superconducting gap (of similar amplitude) in the NbS_2 system as well,[15,16] showing that this interpretation does not hold. Indeed, this isoelectronic compound is particularly interesting to probe for the possible influence of the CDW on the superconducting states in dichalcogenides, as it is the only system among the four 2H layered superconducting transition-metal dichalcogenides[17] MX_2 (M = Nb, Ta; X = S, Se) which does not exhibit a CDW transition. Those measurements hence clearly showed that the presence of two superconducting gaps in 2H-dichalcogenides is not a direct consequence of the presence of a CDW in some of them.

In a first scenario, those two gaps can be considered as being the limiting values of one single anisotropic superconducting gap (without nodes) whereas in an alternative scenario they can be related to different values of the electron-phonon coupling constants ($\lambda_{e\text{-ph}}$) on different sheets of the Fermi surface (FS) (so-called multiband superconductivity[18]).

Clear evidence for multiband superconductivity was first obtained in MgB_2 for which $\lambda_{e\text{-ph}}$ varies from ∼1.2 for the 2 dimensional (2D) σ band to ∼ 0.4 for the 3 dimensional π band.[19,20] Since the FS of $NbSe_2$ is composed of four strongly coupled quasi-2D Nb-derived cylinders (bands 17 and 18 with $\lambda_{e\text{-ph}}$ ranging from 0.8 to 1.9) and one Se-derived pancake sheet with a much smaller $\lambda_{e\text{-ph}}$ value ∼ 0.3 (band 16),[8] it was tempting to ascribe the small superconducting gap to this reduced $\lambda_{e\text{-ph}}$.[21,22] However, angle resolved photo electron spectroscopy (ARPES) measurements[11,14] suggested that, in $NbSe_2$, both gaps open on the tubular sheets and the situation seems to be quite different from that of MgB_2 as the two gaps could both be associated with the same (strongly coupled) FS sheets. However, an experimental confirmation that the two gaps are also related to the same FS sheets in NbS_2 was still lacking.

In order to address this issue, we have performed in-plane penetration depth and penetration field measurements in NbS_2 single crystals. Indeed, λ is a directional probe and corresponding measurements are only sensitive to supercurrents flowing perpendicularly to the direction of the applied magnetic field. Band structure calculations in $NbSe_2$ have for instance shown that the tubular sheets contribute 98% of the transport current in the basal plane,[23] and the present measurements will hence only probe the superconducting properties of those strongly couple sheets. We show here that the temperature dependencies of λ_{ab} are remarkably identical in $NbSe_2$ and NbS_2. This temperature dependence clearly confirms the presence of a small superconducting gap $\Delta_1 = 1.1\,k_BT_c$ (which is much smaller than the standard BCS weak-coupling value) and that, as previously observed in $NbSe_2$, this gap opens on at least one of the Nb sheets. At higher temperature the superfluid density can be deduced from $\lambda(T)$ by introducing a calibration factor (see below) which can be accurately obtained by combining $\lambda(T)$ and first penetration field measurements. We then also show that a second gap value is required to describe the temperature dependence of this superfluid density which can be well described by a two-gap model by introducing gap values very similar to those previously obtained in specific heat measurements. We hence confirm that the presence of two well-defined superconducting gap values, both opening on the Nb tubular sheets, is a generic feature of 2H-dichalconenides.

STS and specific heat (C_p) measurements clearly showed that $NbSe_2$ and NbS_2 systems share the particularity of each having two superconducting gaps but also highlighted some fundamental differences. Indeed, whereas vortices exhibit a clear stellar shape in $NbSe_2$, they appear to be isotropic in NbS_2. Moreover, the two systems have very different anisotropies of their upper critical fields, increasing from $\sim$3.2 in $NbSe_2$[9] to $\sim$8.1 in NbS_2.[24] However, the vortex shape and H_{c2} values are determined by the coherence length (ξ), which is related to the superconducting gap but also to electronic properties of the normal state (Fermi velocity and possibly electronic mean free path in the so-called dirty limit). In contrast, the temperature dependence of the penetration depth is determined only by the superconducting gap structure. Those later measurements hence provide very valuable information to help understand those differences and will be discussed at the end of the paper.

II. SAMPLE AND EXPERIMENTS

H-NbS_2 samples were grown using the vapor transport growth technique with a large sulfur excess, as described elsewhere.[25] Single crystals have a flat hexagonal or triangular shape and typical dimensions of $150^2 \times 30\ \mu$m. The large flat faces grow perpendicular to the c axis. The 2H crystallographic structure has been checked on each sample using a four-circle diffractometer. The bulk critical temperature was checked on several samples of each batch by ac specific heat.[16] All the measured crystals showed sharp superconducting transitions ($\Delta T_c \sim 0.3$ K) at $T_c = (6.05 \pm 0.2)$ K, emphasizing the excellent bulk homogeneity of each crystal. Previous scanning tunneling microscopy measurements on single crystals of the same origin confirmed the absence of a CDW down to 0.1 K.[15] To avoid contamination by oxygen intercalation between layers, which would reduce T_c and smear the transition,[24] samples were kept in vacuum. All the measurements were carried out in the first month following the growth of the samples.

A high-stability LC oscillator operating at 14 MHz, driven by a tunnel diode,[26–28] has been used to measure the variation of the magnetic penetration depth. The tiny sample, placed in the center of the solenoid coil, acts as a small perturbation to the inductance (L). By changing the temperature of the sample, the magnetic penetration depth variations produce a change of the inductance, leading to a change in the LC resonant frequency $\delta f(T)$. The amplitude of the ac excitation field is smaller than 1 μT (that is, $\ll H_{c1}$) to keep the sample in the Meissner state. This technique enables us to measure the variation of λ with an excellent sensitivity as our setup can detect relative frequency changes $\delta f/f_0$ of a few times 10^{-9}, which corresponds to changes in λ on the order of 1 Å in mm^3 samples. The sample is glued with vacuum grease at the bottom of a sapphire cold finger whose temperature is regulated between $T_{\min} = 0.5$ and 10 K whereas the LC oscillator remains at fixed temperature (3 K). The frequency shift $\delta f = f(T) - f(T_{\min})$ is then proportional to the magnetic penetration depth:

$$\delta\lambda(T) = R\frac{\delta f(T)}{\Delta f_0}, \tag{1}$$

where Δf_0 is the change induced by the introduction of the superconducting sample in the coil (measured *in situ* by extracting the cold finger from the coil at the lowest temperature), and R is an effective dimension which depends on the sample geometry. In principle, R can be evaluated by using the formula proposed by Prozorov *et al.*[29] in the case of cylinders. However, recent measurements in pnictides highlighted the difficulties of evaluating this effective dimension, in particular for magnetic fields perpendicular to the ab planes (main sample surface).[30] Indeed, very different $\delta\lambda(T)$ were obtained by different groups, most probably due to the roughness of the sample edges, which undermines this evaluation.

To overcome this difficulty we have performed first penetration field (H_f) measurements using miniature GaAs-based quantum-well Hall probe arrays. The remanent local dc field $[B_{\rm rem}(H_a)]$ in the sample has been measured after applying a magnetic field H_a and sweeping the field back to zero. In the Meissner state, no vortices penetrate the sample and $B_{\rm rem}$ remains equal to zero up to $H_a = H_f$. A finite $B_{\rm rem}$ value is then obtained for $H_a \geqslant H_f$ due to vortices which remain pinned in the sample. As H_f is directly proportional to the first critical field $H_{c1} \propto 1/\lambda^2$, the normalized in-plane superfluid density,

$$\tilde{\rho}_{ab}(T) = \frac{\lambda_0^2}{\lambda_{ab}^2(T)} = \frac{1}{\left[1 + \frac{R}{\lambda_0 \Delta f_0}\delta f(T)\right]^2}, \tag{2}$$

is expected to vary as $H_f(T)/H_f(0)$ (where λ_0 is the zero-temperature penetration depth). Even though the uncertainties on the H_f values hinders any precise determination of the gap values, those measurements can then be used as milestones to obtain the $R/\lambda_0\Delta f_0$ coefficient (see inset of Fig. 3).

III. EVIDENCE FOR A SMALL GAP VALUE IN NbS_2

Figure 1 shows typical $\delta f(T)$ curves between 0.08 T_c and 0.85 T_c for three NbS_2 single crystals (see inset of Fig. 1). The magnetic field is applied perpendicularly to the layers, i.e., along the crystallographic c axis, so that supercurrents are flowing in the layers, probing the in-plane penetration

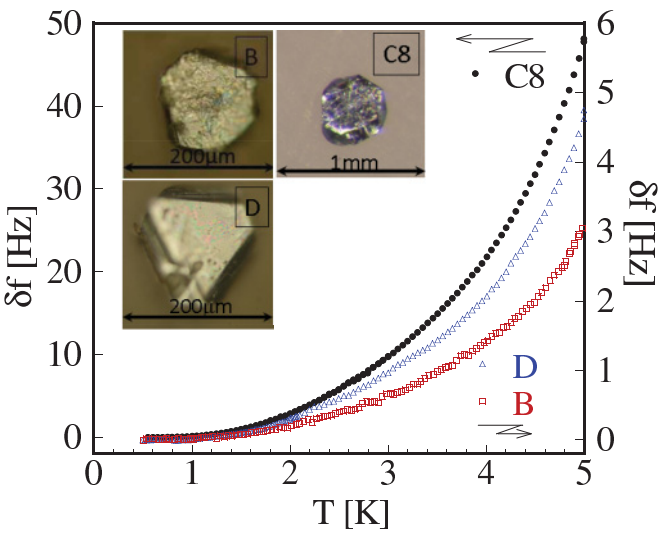

FIG. 1. (Color online) Temperature dependence of the frequency shift δf(T), for B (squares), D (triangles) (right scale), and C8 (circles) (left scale) NbS_2 single crystals. Inset: Microscope images of each sample (with a bigger scale for C8).

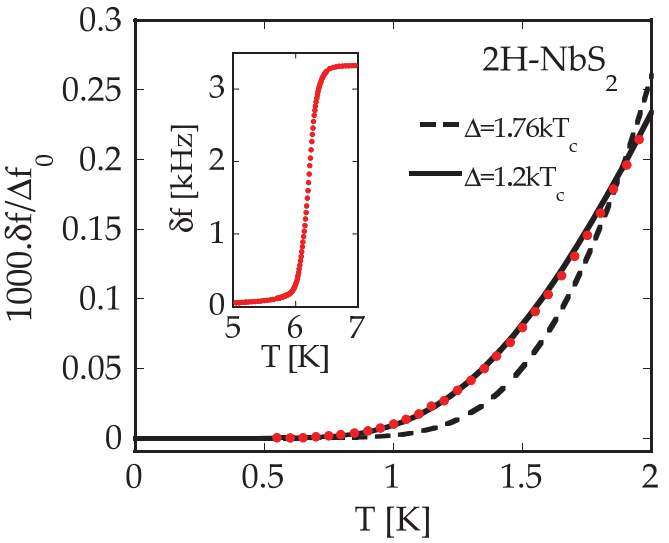

FIG. 2. (Color online) Temperature dependence of the rescaled frequency shift $\delta f/\Delta f_0 \propto \Delta\lambda_{ab}/\lambda_0$ in NbS_2 at $T < T_c/3$ (red circles). Results are fitted with the exponential low-temperature approximation (see text) to determine the smaller gap Δ. An excellent fit is obtained for $\Delta \approx 1.17\, k_B T_c$. Results cannot be described by an exponential behavior with the weak-coupling BCS value $\Delta = 1.76\, k_B T_c$. Inset: Superconducting transition: $T_c = 6.05$ K is determined by the maximum variation of the frequency shift.

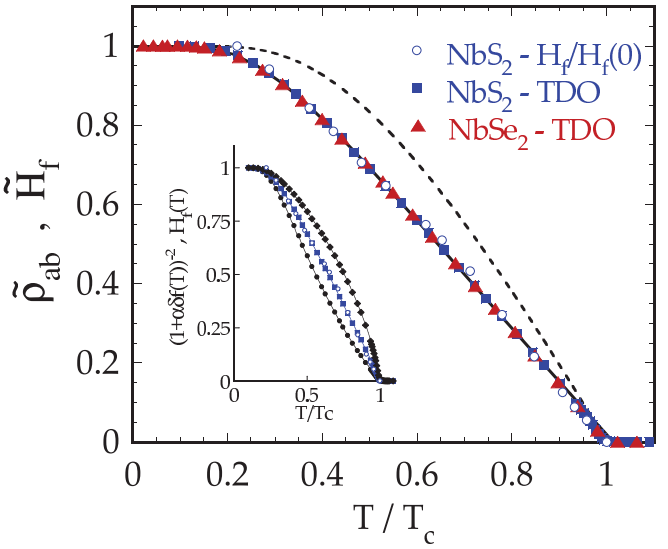

FIG. 3. (Color online) Normalized superfluid density of NbS_2 deduced from tunnel diode oscillator measurements (TDO) for $R\lambda_0/\Delta f_0 = 0.02$ Hz^{-1} (closed squares), compared to $H_f(T)/H_f(0)$ (open circles) both on sample C8. As shown, the weak-coupling BCS normalized superfluid density (dashed line) is not compatible with the data. A very similar temperature dependence was previously obtained in $NbSe_2$ (solid triangles) and both compounds could be well described by a two-gap model (thick line; see text for details). Inset: Influence of the $R/\lambda_0\Delta f_0$ parameter on the shape of the superfluid density, with $R/\lambda_0\Delta f_0$ being equal to, respectively, 0.01, 0.02, and 0.03 Hz^{-1} for diamonds, squares, and circles.

depth, λ_{ab}.[31] Samples B and D were grown in the same batch and have in-plane dimensions equal to 110 and 140 μm, respectively, and thicknesses $t = 30$ and 25 μm, respectively. Sample C8 was grown in a second batch and has a larger size ($430^2 \times 110\ \mu m^3$). The frequency shift is ten times higher for C8 than for other samples due to it larger volume but all renormalized curves are fully identical, underlying the excellent reproducibility of the temperature dependence discussed below.

In the local London theory, at low temperature (typically $T < T_c/3$), the temperature dependence of the gap can be neglected and $\lambda(T)$ is given by

$$(\lambda(T) - \lambda_0)/\lambda_0 = \sqrt{\frac{\pi\Delta(0)}{2k_B T}}\, e^{-\Delta(0)/k_B T}, \qquad (3)$$

where k_B is the Boltzmann constant and $\Delta(0)$ is the value of the smallest superconducting gap at 0 K. Indeed, due to this exponential dependence only the smallest gap is expected to show up at low temperature. As shown in Fig. 2 a very poor agreement to the data is obtained if the gap parameter is fixed to the weak-coupling BCS gap of $1.76 k_B T_c$. A much better fit is obtained by taking $\Delta/k_B = 7.2$ K $\approx 1.2\, T_c$. Note that this gap value does not depend on the renormalization constant. The assumption $\lambda(T_{\min}) \approx \lambda_0$, where $T_{\min}$ is the lowest experimental temperature, is valid here, since an extrapolation of Eq. (3) gives $[\lambda(0.5\text{ K}) - \lambda_0]/\lambda_0 < 10^{-3}$. Since the superfluid current mainly originates from the Nb sheets for $H \| c$, those measurements hence directly show that this small gap is associated with those sheets in NbS_2 as well.

In order to get information on the larger gap, it is necessary to perform a detailed analysis of the temperature dependence at higher temperature. The inset of Fig. 3 displays the temperature dependence of the superfluid density $\tilde{\rho}_{ab}(T)$ up to T_c deduced from Eq. (2) for different $R/\lambda_0\Delta f_0$ values compared to $H_f/H_f(0)$. Note that a small change in $R/\lambda_0\Delta f_0$ will modify strongly the normalized superfluid density, but the curvature of $H_f(T)$ is essentially independent of λ_0. $H_f(T)$ can hence be used to determine $R/\lambda_0\Delta f_0$ with good accuracy and, as shown, a good agreement between H_f and the superfluid density is obtained by taking $R/\lambda_0\Delta f_0 = 0.02$ Hz^{-1}. Clear deviations from the BCS weak-coupling theoretical curve (dashed line) are visible throughout the entire temperature range. In particular, the BCS values exceed the experimental data at low temperature due to the small value of the gap.

In the multigap model, $\tilde{\rho}$ is phenomenologically assumed to be the sum of two independent superfluid densities,

$$\tilde{\rho} = \omega\tilde{\rho}_1 + (1-\omega)\tilde{\rho}_2, \qquad (4)$$

where ω is the weight of band 1 and $\tilde{\rho}_i$ are given by

$$\tilde{\rho}_i(T) = 1 - \int \frac{\partial f}{\partial E}\frac{E}{\sqrt{E^2 - \Delta_i^2(T)}}. \qquad (5)$$

The best fit to the data using Eq. (4) and Eq. (5) (solid line in Fig. 3) is obtained with $\Delta_1 = (1.05 \pm 0.05) k_B T_c$ and $\Delta_2 = (1.8 \pm 0.1) k_B T_c$ with $\omega \sim 0.5$. Those values are in very good agreement with those deduced from tunneling spectroscopy measurements, which revealed a distribution of gaps having two main values at 0.53 meV = 6.15 K $\approx 1\, k_B T_c$ and 0.98 meV = 10.8 K $\approx 1.8\, k_B T_c$.[15] Moreover, the temperature dependence of the specific heat measured on sample C8 can be well described by taking $\Delta_1 \sim 1.05 k_B T_c$, $\Delta_2 \sim 2.1 k_B T_c$,

and $\omega \sim 0.6$.[16] Even if this two-gap model well reproduces the temperature dependence of $\tilde{\rho}_i$ it is worth noting that this temperature dependence is also compatible with a single anisotropic in-plane superconducting gap. The simplest model which respects the symmetry of the crystal has an in-plane six-fold shape, $\Delta(\phi) = \Delta_1 + \frac{\Delta_2 - \Delta_1}{2}[1 + \cos(6\phi)]$, where the extrema of the superconducting gap define two characteristic energy scales. With this model, we find $\Delta_1 \sim 0.9(1) k_B T_c$ and $\Delta_2 \sim 1.9(3) k_B T_c$.

IV. COMPARISON BETWEEN NbS_2 AND $NbSe_2$

We have also reported in Fig. 3 the temperature dependence of $\tilde{\rho}_{ab}$ deduced from penetration depth measurements in 2H-$NbSe_2$.[12] Since the critical temperatures are slightly different in the two compounds, the data have been plotted as a function of T/T_c with $T_c = 6.05$ and 7.1 K for NbS_2 and $NbSe_2$, respectively. In both case, the presence of two characteristic gap values is necessary to fit the temperature dependence of the in-plane superfluid density. We hence show that in both compounds the exotic superconducting gap structure is related to the Nb tubular sheets and that, even if the charge density wave is perturbing those sheets in $NbSe_2$ (but not in NbS_2, which does not exhibit any CDW), this CDW does not affect the superconducting gap structure. Our results hence contradict the ARPES measurements on $NbSe_2$,[11] which suggested a strong correlation between the gap structure and the CDW formation. The presence of an identical exotic gap structure in two different compounds (even of the same family) is particularly rare, highlighting the robustness of the underlying mechanism at its origin. It is worth noting that there exists a $R/\lambda_0 \Delta f_0$ value ($\sim 0.02\ \mathrm{Hz}^{-1}$; see above) for which the temperature dependencies obtained for both compounds are very similar on the whole temperature range.

Note that this strong similitude in the gap structure is not in contradiction with the fact that the vortex cores have an isotropic shape in NbS_2[15] and six-fold shape in $NbSe_2$.[32,33] Indeed, in this later case, the particular shape could be due to an anisotropic Fermi velocity[34] caused by the presence of the charge density wave.

Finally, It is interesting to note that even with similar superconducting gaps, it is possible to understand the large difference of the anisotropy of the upper critical field in the two systems. In the case of $NbSe_2$, the anisotropy of the upper critical field can be understood by the anisotropy of the two set of Nb bands. Indeed, the coherence length related to the pancake band is larger due to a large renormalized Fermi velocity and a small gap.[8] According to band structure calculations, the anisotropies of the Fermi velocities (v_F^{ab}/v_F^c) of the two tubular sheets are on the order of 2 (Band 17[35]) and 10 (Band 18) in $NbSe_2$, neither of which corresponds to the experimental value of the anisotropy of the upper critical field (~ 3.2)[23]. However, $\mu_0 H_{c2}^{\parallel c}(0) = \Phi_0/2\pi\xi_{ab}^2$ is defined by the band having the smallest ξ_{ab} value. All bands have quite similar in-plane Fermi velocities but if one assumes that Δ_2 is associated with band 17 and Δ_1 is associated with band 18, one gets $\xi_{ab,17} \sim (\Delta_1/\Delta_2)\xi_{ab,18} \sim \xi_{ab,18}/1.7$ and $H_{c2}^{\parallel c}$ will be defined by band 17. Moreover, for $\mu_0 H_{c2}^{\parallel ab}(0) = \Phi_0/2\pi\xi_{ab}\xi_c$, the very small value of c-axis Fermi velocity of band 18 implies that $H_{c2}^{\parallel ab}$ will be defined by this latter band. One hence gets $H_{c2}^{\parallel ab}/H_{c2}^{\parallel c} = (v_F^{ab,17} v_F^{ab,17}/v_F^{ab,18} v_F^{c,18})(\Delta_1/\Delta_2)^2 \sim 10/(1.7)^2 \sim 3$, in good agreement with the experimental value. Note that this situation strongly differs from the one observed in MgB_2 in which the anisotropy of H_{c2} is defined only by the σ band (for $T \ll T_c$). As $NbSe_2$ and NbS_2 have similar $H_{c2}^{\parallel ab}$ values, one can conclude that band 18 is not affected by the chemical substitution and the increase of the H_{c2} anisotropy to ~ 8.1 in NbS_2 is hence due to an increase of $v_F^{ab,17}$ but this change in the Fermi velocity does not affect the superconducting gap structure.

The presence of two characteristic gap values appears to be a robust characteristic feature in 2H dichalcogenides, but its origin is still open to questions. With the present results, the influence of the CDW also has to be excluded, underlying the necessity of proposing new clues for the origin of the reduced superconducting gap observed in both compounds.

V. CONCLUSION

The temperature dependence of the in-plane magnetic penetration depth of single crystals of 2H-NbS_2 has been measured and compared to previous measurements on 2H-$NbSe_2$. The temperature dependence shows a similar curvature in both compounds, evidencing a similar reduced superconducting gap structure in the sheets of the Fermi surface where the e-ph coupling constant is the largest. The CDW, present only in $NbSe_2$, is not at the origin of the reduced superconducting gap. In the light of the discovery of a particular acoustic phonon mode observed in lead or niobium,[36] more accurate knowledge of the phonon dispersion in NbS_2 could shed insight into the origins of the reduced superconducting gap in the dichalcogenides.

ACKNOWLEDGMENTS

P.R. thanks R. and B. Thomas for helpful discussions. T.K. is most obliged to V. Mosser of ITRON, Montrouge, and M. Konczykowski from the Laboratoire des Solides Irradiés, Palaiseau, for the development of the Hall sensors used in this study.

[1] G. Seyfarth, J. P. Brison, G. Knebel, D. Aoki, G. Lapertot, and J. Flouquet, Phys. Rev. Lett. **101**, 046401 (2008).
[2] E. Morosan, H. W. Zandbergen, and B. S. E. A. Dennis, Nature Phys. **2**, 544 (2006).
[3] A. F. Kusmartseva, B. Sipos, H. Berger, L. Forro, and E. Tutis, Phys. Rev. Lett. **103**, 236401 (2009).
[4] B. Sipos *et al.*, Nature Mater. **7**, 960 (2008).
[5] K. E. Wagner *et al.*, Phys. Rev. B **78**, 104520 (2008).
[6] P. Garoche, J. J. Veyssié, P. Manuel, and P. Molinié, Solid. State Commun. **19**, 455 (1976).
[7] H. F. Hess, R. B. Robinson, R. C. Dynes, J. M. Valles, and J. V. Waszczak, Phys. Rev. Lett. **62**, 214 (1989).

[8]R. Corcoran, P. Meeson, Y. Onuki, P. A. Probst, M. Springford, K. Takita, H. Harima, G. Y. Guo, and B. L. Gyorffy, J. Phys. Condens. Matter **6**, 4479 (1994).
[9]D. Sanchez, A. Junod, J. Muller, H. Berger, and F. Lévy, Physica B **204**, 167 (1995).
[10]I. Guillamon, H. Suderow, F. Guinea, and S. Vieira, Phys. Rev. B **77**, 134505 (2008).
[11]T. Kiss, T. Yokoya, A. Chainani, S. Shin, T. Hanaguri, M. Nohara, and H. Takagi, Nature Phys. **3**, 720 (2007).
[12]J. D. Fletcher, A. Carrington, P. Diener, P. Rodiere, J. P. Brison, R. Prozorov, T. Olheiser, and R. W. Giannetta, Phys. Rev. Lett. **98**, 057003 (2007).
[13]A. H. Castro Neto, Phys. Rev. Lett. **86**, 4382 (2001).
[14]S. V. Borisenko *et al*., Phys. Rev. Lett. **102**, 166402 (2009).
[15]I. Guillamon, H. Suderow, S. Vieira, L. Cario, P. Diener, and P. Rodiere, Phys. Rev. Lett. **101**, 166407 (2008).
[16]J. Kacmarcik, Z. Pribulova, C. Marcenat, T. Klein, P. Rodiere, L. Cario, and P. Samuely, Phys. Rev. B **82**, 014518 (2010).
[17]R. Friend and A. D. Yoffe, Adv. Phys. **36**, 1 (1987).
[18]H. Suhl, B. T. Matthias, and L. R. Walker, Phys. Rev. Lett. **3**, 552 (1959).
[19]H. Choi, D. Roundy, H. Sun, M. Cohen, L. Louie, and G. Steven, Nature (London) **418**, 758 (2002).
[20]I. I. Mazin and V. P. Antropov, Physica C **385**, 49 (2003).
[21]T. Yokoya *et al*., Science **294**, 2518 (2001).
[22]E. Boaknin *et al*., Phys. Rev. Lett. **90**, 117003 (2003).
[23]M. D. Johannes, I. I. Mazin, and C. A. Howells, Phys. Rev. B **73**, 205102 (2006).
[24]K. Onabe, M. Naito, and S. Tanaka, J. Phys. Soc. Jpn. **45**, 50 (1978).
[25]W. Fisher and M. Sienko, Inorg. Chem. **19**, 39 (1980).
[26]C. Van Degrift, Rev. Sci. Instrum. **46**, 599 (1975).
[27]P. Diener, P. Rodiere, T. Klein, C. Marcenat, J. Kacmarcik, Z. Pribulova, D. J. Jang, H. S. Lee, H. G. Lee, and S. I. Lee, Phys. Rev. B **79**, 220508 (2009).
[28]R. Prozorov, R. W. Giannetta, A. Carrington, P. Fournier, R. L. Greene, P. Guptasarma, D. G. Hinks, and A. R. Banks, Appl. Phys. Lett. **77**, 4202 (2000).
[29]R. Prozorov, R. W. Giannetta, A. Carrington, and F. M. Araujo-Moreira, Phys. Rev. B **62**, 115 (2000).
[30]T. Klein, D. Braithwaite, A. Demuer, W. Knafo, G. Lapertot, C. Marcenat, P. Rodiere, I. Sheikin, P. Strobel, A. Sulpice, and P. Toulemonde, Phys. Rev. B **82**, 184506 (2010).
[31]B. S. Chandrasekhar and D. Einzel, Ann. Phys. **2**, 535 (1993).
[32]H. F. Hess, R. B. Robinson, and J. V. Waszczak, Phys. Rev. Lett. **64**, 2711 (1990).
[33]I. Guillamon, H. Suderow, S. Vieira, and P. Rodiere, Physica C **468**, 537 (2008).
[34]F. Gygi and M. Schluter, Phys. Rev. Lett. **65**, 1820 (1990).
[35]The two set of Nb bands, called 17 and 18 by Corcoran *et al*., correspond, respectively, to 2 and 3 in Johannes and Mazin.
[36]P. Aynajian, T. Keller, L. Boeri, S. M. Shapiro, K. Habicht, and B. Keimer, Science **319**, 1509 (2008).